P- ISSN 1991-8941 E-ISSN 2706-6703
2020,14 (2): 55-63

Journal of University of Anbar for Pure Science (JUAPS)

Open Access

Hysteresis Loop Effect on Intensity for Horizontal and Vertical Polarization by Optical Feedback

Ehsan Ali Abed[*1,2], Jassim Mohammed Najim[1], and Suaded Salman Ahmed[3]

[1] Department of Physics, College of Science, University of Anbar, Iraq
[2] Department of Basic Sciences, College of Dentistry, University of Anbar, Iraq
[3] Department of Physics, College of Science, University of Baghdad, Iraq

ARTICLE INFO

Received: 16 / 5 /2020
Accepted: 7 / 6 / 2020
Available online: 1 / 12 / 2020

DOI: 10.37652/juaps.2022.172388

Keywords:
Hysteresis loop, Optical feedback, Polarization, He-Ne laser.

ABSTRACT

The effect of optical feedback on hysteresis loop (HL) is investigated. Hysteresis loop occurs between two eigenstates of the He-Ne laser (x , y) and it changes by optical feedback at angles from 0° to 180°. Hysteresis loop size decreases and increases with the rotation angle (θ) of the polarization. Hysteresis loop effects on vertical (⊥) and horizontal (//) polarization and the intensity for two eigenstates. When HL size increases, then the intensity ($I_{\perp}$ or $I_{//}$) decreases vice versa clear. Best results at 70-110 angles from the external cavity (optical feedback cavity), whereas the intensity very high and HL disappear.

1. INTRODUCTIN

Polarization of light: when the direction of the electric field of light oscillates in an ordinary unsurprising style, then the light is polarized. Polarization depicts the direction of the oscillating electric field, whereas if the direction of the electric field of light oscillates rapidly and randomly, then the light is unpolarized [1]. He-Ne laser oscillates in two orthogonally polarized modes in the resonant cavity, the first //-mode represents horizontal polarization and the second ⊥-mode represents vertical polarization [2]. The polarization flipping forms transform into an invader laser in case an inside factor, for example, the laser frequency is different [3].

There are two mechanisms involved in polarization flipping; the rotation mechanism and the inhibition mechanism [2]. Light hysteresis or hysteresis loop is generate by two mechanism.Via reflecting piece of the laser yield once more into the ringing cavity, the conduct of the laser, particularly the constant with effective characteristics, may be fundamentally influenced, after the total or partial electric field reflects from the external cavity mirror into the intra cavity will be occurs interference between the electric field from the intra cavity and the electric field from the external cavity leads to the gain and intensity modulated,

Also, this interference effects on vertical and horizontal polarization (polarization modes), that is known as the optical feedback impact, or self-blending intervention, which was first announced by King and Steward [4-9].

In this paper, we study the hysteresis loop effect on intensity modulation for horizontally and vertically polarization with angle from polarizer rotating in external cavity by optical feedback.

1.1. Theoretical Part

The two modes polarizations rely upon the dynamic middle, a linear stage contrast, a wastage contrast and feedback stage from external cavity. When $\Delta\Phi_{xy}$ phase-anisotropy values are small, then the polarization flipping occurs by the rotation mechanism [3]. The polarization overturn case of x to y, may be written as

$$\left[-\frac{1}{2}\frac{\rho_+}{\beta_+}\Delta\Phi_{xy}\right]+\left[\frac{c}{L}\frac{1}{4\alpha_+}\frac{S+1}{2S}\Delta\Phi_{xy}^2\right]+\frac{1}{2}\left[\frac{t_y}{t_x}-1\right]>0 \ldots\ldots(1)$$

Where the proportion ρ_+/β_+ of the dispersive and absorptive nonlinear coefficients against the frequency,α_+ is laser net gain, **S**= -3/20 for a J=1→J=2 transmission, $\Delta\Phi_{xy}$ is the stage contrast into inner bore, t_y with t_x constitute the transition factors of horizontal with vertical polarization. The initial expression of equation (1) clarifies the impact of the energetic middle, the second expression clarifies the impact of the linear stage contrast of inner bore while the

*Corresponding author at: Department of physics, College of Science, University of Anbar, Ramadi, Iraq. Tel.: +964 7822306487; G-mail address:abedehsan202@gmail.com

tertiary expression clarifies the impact of the wastage contrast.

With the existence of optical feedback and according to the model of tantamount cavity of Fabry-Perot interferometer, then the equivalent mirror reflectivities along x-axis and y-axis can be given by means of [10].

$$R_x = R_2 + 2M_{//}(R_2R_3)^{1/2}(1-R_2)cos\varphi_f \dots\dots(2)$$

$$R_y = R_2$$

$$M_{\parallel} = cos^4\theta + sin^2 2\theta/4$$

$$(\frac{R_y}{R_x})^{\frac{1}{2}} \approx 1 - 2M_{//}(\frac{R_3}{R_2})^{\frac{1}{2}}(1-R_2)cos\varphi_f \dots\dots\dots\dots\dots(3)$$

Where $\varphi_f=4\pi l/\lambda$ clarifies the stage of exterior bore, $M_{//}$ is the factor prompted via jones matrix of polarizer and l: represents the length of exterior bore.

Via letting $\frac{t_y}{t_x} = (\frac{R_y}{R_x})^{1/2}$

Substituting Eq. (3) into Eq.(1), the case of polarization overturn of x to y may be written as

$$\left[-\frac{1}{2}\frac{\rho_+}{\beta_+}\Delta\Phi_{xy}\right] + \left[\frac{c}{L}\frac{1}{4\alpha_+}\frac{S+1}{2S}\Delta\Phi_{xy}^2\right] + \frac{1}{2}\left[1 - 2M_{//}(\frac{R_3}{R_2})^{\frac{1}{2}}(1-R_2)cos\varphi_f - 1\right] > 0 \dots\dots\dots(4)$$

$$\left[-\tfrac{1}{2}\tfrac{\rho_+}{\beta_+}\Delta\Phi_{xy}\right] + \left[\tfrac{c}{L}\tfrac{1}{4\alpha_+}\tfrac{S+1}{2S}\Delta\Phi_{xy}^2\right] + \left[-M_{//}kcos\varphi_f\right] > 0 \dots\dots\dots\dots(5)$$

Where $k = (\frac{R_3}{R_2})^{\frac{1}{2}}(1-R_2)$

$$\left[-\tfrac{1}{2}\tfrac{\rho_+}{\beta_+}\Delta\Phi_{xy}\right] + \left[\tfrac{c}{L}\tfrac{1}{4\alpha_+}\tfrac{S+1}{2S}\Delta\Phi_{xy}^2\right] > M_{//}kcos\varphi_f \dots\dots\dots\dots(6)$$

Due to the fact that the frequency shift resulting from optical feedback with the inner bore contrast is very little[11], if we forget gratification consequences, Equations(2) with (6) Display that the vertex of polarization might be along the bigger reflexivity axis, and the right expression in equation (6) may be supposed as zero. In this situation, the light can be polarized along x-pivot ($M_{//}\cos\varphi_f > 0$) or y-pivot ($M_{\perp}\cos\varphi_f < 0$). While polarization course of laser is for a long way x- pivot, the intensity changes may be received via using [12]

$$\Delta I_x = \eta M_{//}cos\varphi_f \dots\dots(12)$$

In which η clarifies the optical feedback component.

The y to x overturn case is just like equation (1), and only the marks of the initial and tertiary expressions are modified. The case of polarization overturn of y to x may be as follows;

$$\left[\frac{1}{2}\frac{\rho_+}{\beta_+}\Delta\Phi_{xy}\right] + \left[\frac{c}{L}\frac{1}{4\alpha_+}\frac{S+1}{2S}\Delta\Phi_{xy}^2\right] - \frac{1}{2}\left[\frac{t_y}{t_x} - 1\right] > 0 \dots\dots\dots(8)$$

Similarly, while the polarization trend of laser is paralleled to y- pivot, the tantamount mirror reflexivities for a long way y- pivot and x- pivot are may be as follows;

$$R_y = R_2 + 2M_{\perp}(R_2R_3)^{1/2}(1-R_2)cos\varphi_f \dots\dots\dots\dots\dots(9)$$

$$R_x = R_2$$

$$M_{\perp} = sin^4\theta + sin^2 2\theta/4$$

$$\frac{R_y}{R_x} = 1 + 2M_{\perp}(\frac{R_3}{R_2})^{\frac{1}{2}}(1-R_2)cos\varphi_f \dots\dots\dots\dots\dots(10)$$

By letting $\frac{t_y}{t_x} = \frac{R_y}{R_x}$

Replacing equation (10) in equation (8), we will be able to get the situation of polarization overturn from y to x

$$\left[\frac{1}{2}\frac{\rho_+}{\beta_+}\Delta\Phi_{xy}\right] + \left[\frac{c}{L}\frac{1}{4\alpha_+}\frac{S+1}{2S}\Delta\Phi_{xy}^2\right] - \frac{1}{2}\left[1 + 2M_{\perp}(\frac{R_3}{R_2})^{\frac{1}{2}}(1-R_2)cos\varphi_f - 1\right] > 0 \dots\dots\dots(11)$$

$$\left[\frac{1}{2}\frac{\rho_+}{\beta_+}\Delta\Phi_{xy}\right] + \left[\frac{c}{L}\frac{1}{4\alpha_+}\frac{S+1}{2S}\Delta\Phi_{xy}^2\right] - \left[M_{\perp}kcos\varphi_f\right] > 0 \dots\dots(12)$$

$$\left[\frac{1}{2}\frac{\rho_+}{\beta_+}\Delta\Phi_{xy}\right] + \left[\frac{c}{L}\frac{1}{4\alpha_+}\frac{S+1}{2S}\Delta\Phi_{xy}^2\right] > \left[M_{\perp}kcos\varphi_f\right] \dots\dots(13)$$

The light can be polarized for a long way y- pivot ($M_{\perp}\cos\varphi_f$ greater from zero) or x- pivot ($M_{//}\cos\varphi_f$ less from zero). If Polarization trend of laser is for a long way y-pivot, the intensity alteration is

$$\Delta I_y = \eta M_{\perp}cos\varphi_f \dots\dots(14)$$

When $\Delta\Phi_{xy}$ anisotropy values are greater, then the polarization flipping occurs by the inhibition mechanism [3]. The variations among the ringing hesitations are too massive with the oscillators E_x and E_y are not closed collectively. Thus, at some stage in the flip, two oscillators vibrate concurrently at hesitations ν_x with ν_y respectively. The time conduct of the eigenstates capacities may be written down in a shape originated from Lamb's theorem [13-16],

$$\dot{E_x} = E_x(\alpha_x - \beta_x E_x^2 - \theta_{xy}E_y^2) \dots\dots(15)$$

$$\dot{E_y} = E_y(\alpha_y - \beta_y E_y^2 - \theta_{yx}E_x^2) \dots\dots(16)$$

Where α_x with α_y are the pure earn factors and β_x , β_y and θ_{xy} , θ_{yx} the self- with pass- gratification factors. The constant-case solution for the capacity of the two contending eigenstates may be related, as is the case in a laser with two linear styles with a potential [17],

$$V(E_x, E_y) = -\frac{1}{2}\alpha_x E_x^2 - \frac{1}{2}\alpha_y E_y^2 + \frac{1}{4}\beta_x E_x^4 + \frac{1}{4}\beta_y E_y^4 + \frac{1}{2}\theta_{xy} E_x^2 E_y^2 \dots\dots\dots (17)$$

This type of potential allows us to illustrate the full order with the spatial graph of figure1 (a) [18].

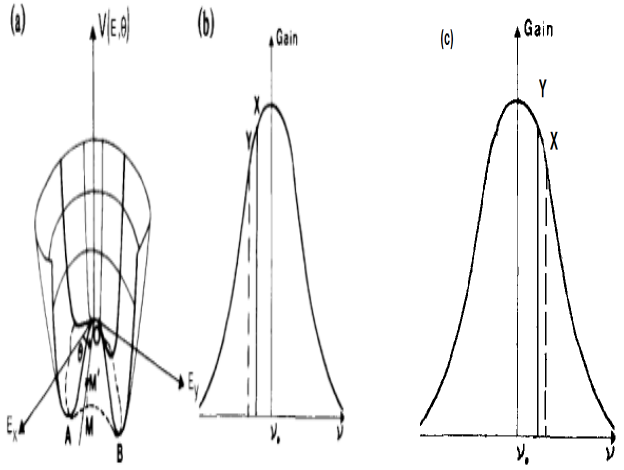

Fig:1: (a) Spatial illustration of the popularized potentials. (b) and (c) Position of x with y eigenstates.

This potential on two pivots (x , y) decreases to

$$V(E) = -\frac{1}{2}\alpha E^2 + \frac{1}{4}\beta E^4 \dots\dots (18)$$

With regard to the traditional laser with a monosyllabic vibrating eigenstate. While the decay of the eigenstate hesitations is eliminated through an inner bore double refraction, the harmony of the laser hesitation through the earn curve, figure1-b and c, allows us to differentiate the proportional altitudes of the operating dots *A* with *B*. A realization of the eigenstate dynamics versus the hesitation reliance is then feasible. This easy spatial graph indicates twain of prospects for the eigenstate dynamics. The system might transit from A to B utilizing two trajectories: (i) The electric field rotates*(*rotation mechanism) in the transversal plane, the system moving along the AMB streak with a hesitation driftage, (ii) A mode inhibition(inhibition mechanism) takes place along the AOB path. The two points A and B both wells similar to the x and y eigenstates, respectively.

At state rotation mechanism, the laser oscillates first of all at the x eigenstate. The working dot is in the well A as figure 3(a) shows. We observe the presence of another well B conformable with the non-vibrating y eigenstate. The two wells A and B are detached through a potential bulkhead resulting from the rotation damages Δp(θ)

$$\Delta \boldsymbol{p}(\boldsymbol{\theta}) \approx 8\Delta\Phi_{xy}^2 \frac{\left[\theta^2 cos^2\theta + (\pi/_2 - \theta)^2 sin^2\theta\right]}{\pi^2} \dots\dots (19)$$

Δp(θ relies on the rotation angle (θ) of the polarization from the x pivot. If the prorated altitudes of A and B are numerous via means of growing the laser hesitation for example, the polarization is able to rotate from x to y [Figure 3(b)], it is the y eigenstate which presently vibrates. The presence of those two potential wells A and B is linked to the two various command coefficients E_x and E_y, which denotes that the rotation of the polarization corresponds to a first-command stage transmission and so happens with hysteresis when the laser hesitation is examined [3].

In case of inhibition mechanism, the barrier among the two wells A and B is produced in this situation to a robust conjugation value

$$C = \frac{\theta_{xy}\theta_{yx}}{\beta_x\beta_y} > 1 \dots\dots\dots\dots (20)$$

The differences among the proportional altitudes of A and B acquired by way of wiping the laser hesitation give a mode inhibition. At some point of the x to y overturn as an example, the x eigenstate vibrating at frequency ν_x turns off even as concurrently the y eigenstate turns on at a various hesitation ν_y. The existence of this bulkhead concerning the two command coefficients denotes that the inhibition mechanism corresponds also to a first- command stage transmission and takes place with hysteresis.

Subsequent to Lamb's construes utilized for a laser with two longitudinal styles with the same linear polarization, the situation for the overturn from x to y is recorded as in [13,14]

$$\alpha_y - \theta_{yx} I_x > 0 \dots\dots\dots\dots (21)$$

$$I_x = \frac{\alpha_x}{\beta_x} \dots\dots\dots\dots\dots\dots (22)$$

Where I_x is the intensity of the x vibrating eigenstate. This case leads to the y eigenstate structure if its pure earn α_y is great enough in order to overcome the competition expression $\theta_{yx}I_x$. In a different verbalism, this last expression clarifies the self-constancy of the x lasing eigenstate to impede the beginning of the y eigenstate. In a comparable method, the y-to-x overturn situation is

$$\alpha_x - \theta_{xy} I_y > 0 \dots\dots (23)$$

$$I_y = \frac{\alpha_y}{\beta_y} \dots\dots\dots\dots\dots\dots (24)$$

Where I_y is the intensity of the y vibrating eigenstate. The various coefficients appearing within the sip conditions (21) and (23) have been calculated in [16]. The pure earn α_i (i = x, y) is recorded as

$$\alpha_i = \alpha_0 exp\left[-\left(\frac{\nu_i - \nu_0}{\Delta\nu_D/2}\right)^2\right] - p_i \dots\dots\dots\dots (25)$$

In which pi clarifies the rate damages per second of the eigenstate i, α_0 is the unsaturated earn coefficient for the field capacity at the ringing hesitation of the atomic transition ν_0, and $\Delta\nu_D$ is the full Doppler width at 1/e. The self-saturation β_i is

$$\beta_i = \beta_0[1 + L(\nu_0 - \nu_i)]exp\left[-(\frac{\nu_i - \nu_0}{\Delta\nu_D/2})^2\right] \ldots..(26)$$

where β_0 distinguishes the self-saturation at line middle and depends at the atomic coefficients and at the irritation. The Lorentzian L is determined by using

$$L(\nu_0 - \nu_i) = \frac{\gamma^2}{[\gamma^2+(\nu_0-\nu_i)^2]} \ldots\ldots\ldots(27)$$

Where γ is the homogeneous width of the transmission [half width at half maximum (HWHM)]. The cross-saturation parameter θ_{ij} may be written if we forget spatial puncture combustion influences [13,14],

$$\theta_{ij} = \theta_0\left[L\left(\frac{\Delta\nu_{xy}}{2}\right) + L(\nu_0 - \frac{\nu_i}{2} - \frac{\nu_j}{2})\right]exp\left[-(\frac{\nu_i - \nu_0}{\Delta\nu_D/2})^2\right] \ldots\ldots\ldots(28)$$

For $\Delta\nu_{xy} << 2\gamma$, i.e. for small double refraction values the expression of θ_{ij} decreases to

$$\theta_{ij} \approx \theta_0[1 + L(\nu_0 - \nu_i)]exp\left[-(\frac{\nu_i - \nu_0}{\Delta\nu_D/2})^2\right] \ldots\ldots\ldots(29)$$

so that an inhibition term such as $\theta_{xy}I_x$ emerges using (26) and (29) as follows;

$$\theta_{yx}I_x = (\theta_0/\beta_0)\alpha_x \ldots\ldots(30)$$

The coupling constant may be recorded as

$$C = \frac{\theta_{xy}\theta_{yx}}{\beta_x\beta_y} \approx (\frac{\theta_0}{\beta_0})^2 \ldots\ldots\ldots\ldots..(31)$$

and the previous disparities (21) and (23) lead thereafter to the subsequent approached x-to-y and y-to-x overturn conditions:

$$\alpha_{y,x} - \sqrt{C}\alpha_{x,y} > 0 \ldots\ldots\ldots(32)$$

Because the coupling consistent C among the two eigenstates is robust, i.e., C >1, this denotes vectorial bistability [19]. Idiom (31) can nonetheless be utilized if we keep in mind that the speed-converting collides are enough to interpret the major features of the inhibition mechanism.

2.EXPERIMENTAL PART

The format of empirical settings is exhibited in Fig. 2. The settings include three portions: feedback portion, laser, and detection portion.

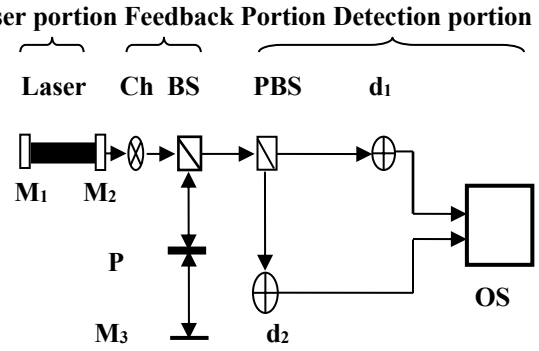

Fig:2: The format of empirical settings and main coordinates. M_1, M_2 cavity mirrors; Ch, chopper; BS, beam splitter; P, polarizer; M_3, feedback mirror; PBS, polarizing ray splitter; d_1, d_2, detectors; OS, digital storage oscilloscope.

The intra-cavity He-Ne laser produces linear polarization with a monocular longitudinal style vibrating in the ringing bore, the running wavelength is 632. 8 nm. The gassy compression proportions inside the laser igniter are He: Ne = 9:1 and Ne20: Ne22 = 1:1. The reflexivities of bore mirrors M_1 and M_2 are 99.99% and 99%, respectively. The length of the ringing bore created by way of mirror M_1 and M_2 is 40 cm. The total intensity for He-Ne laser is 4mW without chopper and it is with chopper 2.5mW. The intensity reaches to M_3 is 1.25Mw and it same value reaches to PBS.The Feedback portion is consist of chopper Ch., feedback mirror M_3, and polarizer P. The Feedback bore length is nearly 60 cm. The reflectivity of M_3 is 99.99%. The angle among x pivot and the optical pivot of P is indicated by way of θ. The light whose polarization is parallal to x pivot is indicated by using //-polarization, and the other one is indicated with the aid of ⊥-polarization. The detection portion includes the polarizing beam splitter PBS, photo detectors d_1, d_2, and OS, digital storage oscilloscope. The vertical polarization (⊥) and horizontal polarization (//) are detached through PBS, and their intensities vertical ($I_\perp$) and horizontal ($I_{//}$) are revealed by d_1 , d_2 and OS respectively.

3. RESULTS AND DISCUSSION

From Fig. 3, we can see that the hysteresis loop (HL) and the polarization flipping between horizontal (//) and vertical (⊥) polarization are obtained without and with optical feedback. From fig. 3(a), // and ⊥ polarization without optical feedback, we observe $I_{//}$ and $I_\perp$ are stable and the hysteresis loop (HL) is constant because of absence of the optical feedback. In Fig. 3(b) at θ=0° only //-polarization oscillates and $I_{//}$ is modulated by optical feedback because of the overlap between $\mathbf{E}_{//ext.}$ and $\mathbf{E}_{//int.}$ into intra cavity and the hysteresis loop (HL) is low at the

polarization flipping from x-to-y. When ⊥-polarization does not oscillate, $I_{\perp}$ is stabilized because of the existence of the polarizer. At θ=10º,20º (figures 3c and 3d) $I_{//}$ increase and the hysteresis loop is low because of the optical feedback. At θ=25º, 30º (figures 3e and 3f) only ⊥- polarization oscillates and $I_{\perp}$ increases because of the overlap between $\mathbf{E}_{\perp ext.}$ and $\mathbf{E}_{\perp int.}$ into intra cavity. At θ=40º(figure 3g), the polarization flipping from y-to-x is obtained and $I_{\perp}$ increases and the hysteresis loop is low. At θ=50º, 60º, 70º, 80º, 90º (figures 3h, 3i, 3j, 3k and 3l) $I_{\perp}$ increases and the hysteresis loop is low.

$I_{\perp}$ is higher than $I_{//}$ with optical feedback and the hysteresis loop at //- polarization oscillates does not disappear while at ⊥-polarization oscillates it disappears.

At θ=100º, 110º ,120º , 130º, 140º, 145º (figures 3m, 3n, 3o, 3p, 3q and 3r) only ⊥-polarization oscillates , $I_{\perp}$ decreases to reach pre-feedback and the hysteresis loop increases, while //- polarization does not oscillate. At θ=150º,160º,170º (figures 3s, 3t, and 3u) $I_{\perp}$ and $I_{//}$ together decrease to reach pre-feedback. At θ=175º,180º(figures 3v and 3w) only //- polarization oscillates and ⊥-polarization does not oscillate, the polarization overturns from x to y and hysteresis loop decreases.

The polarization overturn from y to x occurs at θ=100º-130º, while from x to y it occurs at θ=135º-180º.

With the existence of optical feedback, consistent with self-consistency of standing wave bore, the re-injection of light will give rise to an alteration within the sill earn of the laser [20], therefore $I_{//}$ and $I_{\perp}$ are increased with optical feedback.

Vertical and horizontal intensities are increased and the hysteresis loop is decreased with optical feedback because of the inhibition mechanism, whereas $I_{//}$ and $I_{\perp}$ are decreased and the hysteresis loop is increased with optical feedback because of the rotation mechanism.

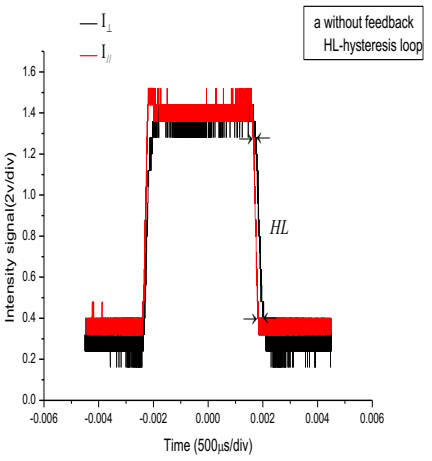

Fig:3.a: $I_{\perp}$ and $I_{//}$ intensity without optical feedback(OFB)

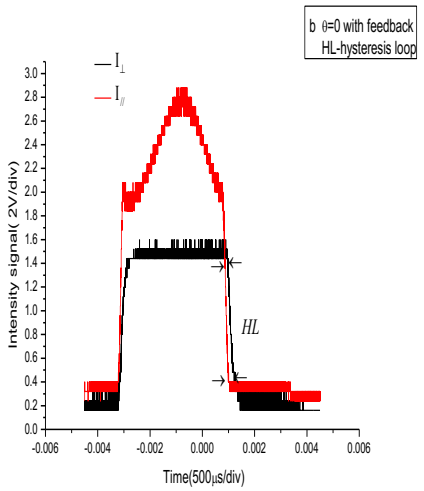

Fig:3.b: $I_{\perp}$ and $I_{//}$ intensity with OFB at θ=0º

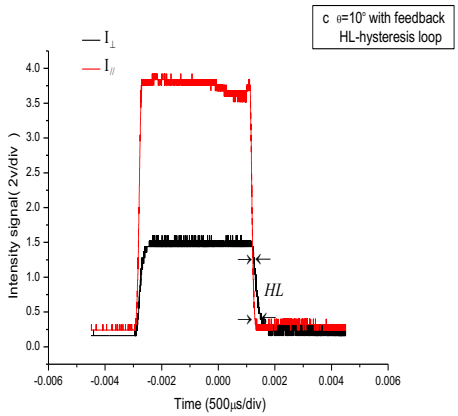

Fig:3.c:$I_{\perp}$ and $I_{//}$ intensity with OFB at θ=10º

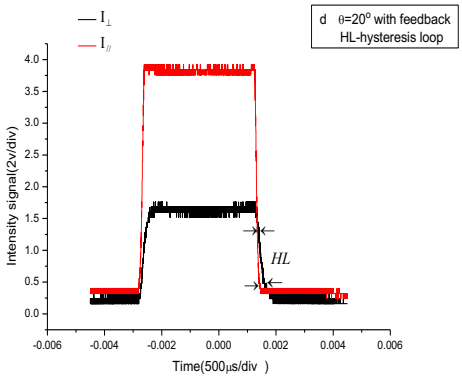

Fig:3.d: $I_{\perp}$ and $I_{//}$ intensity with OFB at θ=20º

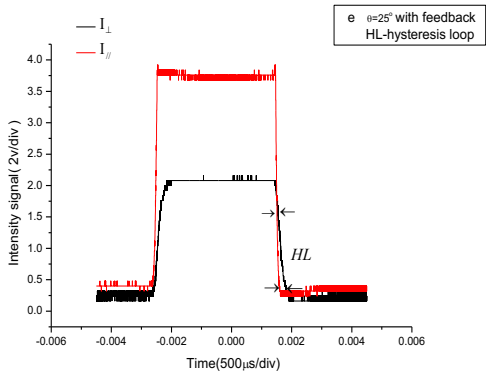

Fig:3.e: $I_{\perp}$ and $I_{//}$ intensity with OFB at θ=25°

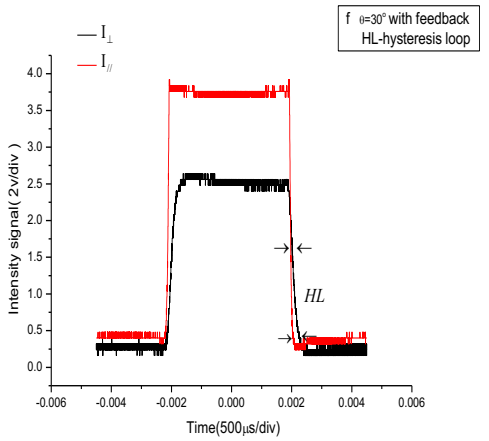

Fig:3. f: $I_{\perp}$ and $I_{//}$ intensity with OFB at θ=30°

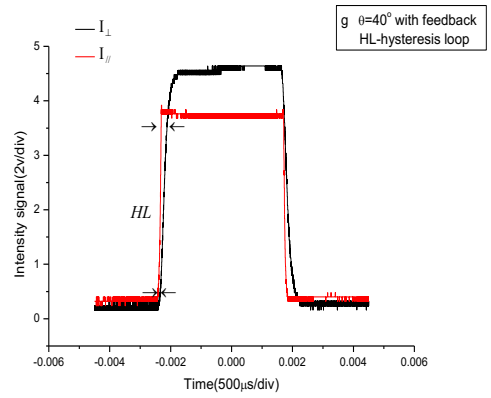

Fig:3.g: $I_{\perp}$ and $I_{//}$ intensity with OFB at θ=40°

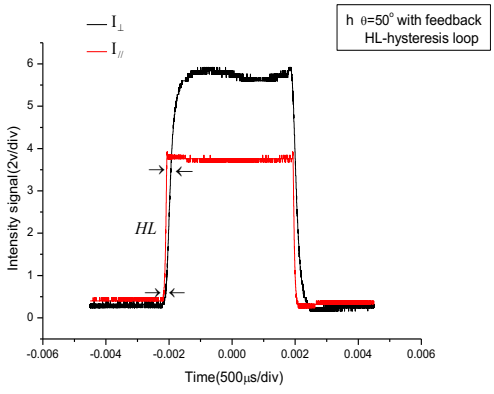

Fig:3.h: $I_{\perp}$ and $I_{//}$ intensity with OFB at θ=50°

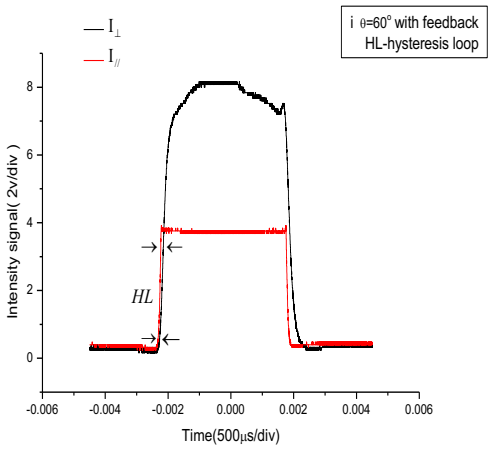

Fig:3.i: $I_{\perp}$ and $I_{//}$ intensity with OFB at θ=60°

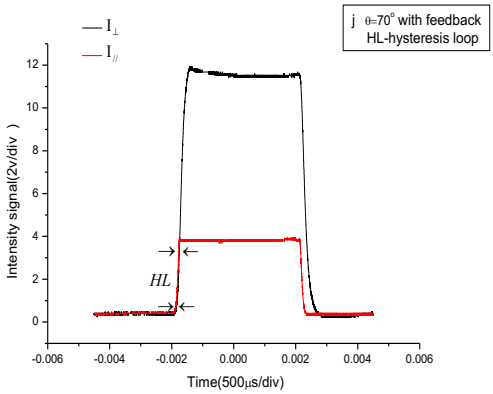

Fig:3.j: $I_{\perp}$ and $I_{//}$ intensity with OFB at θ=70°

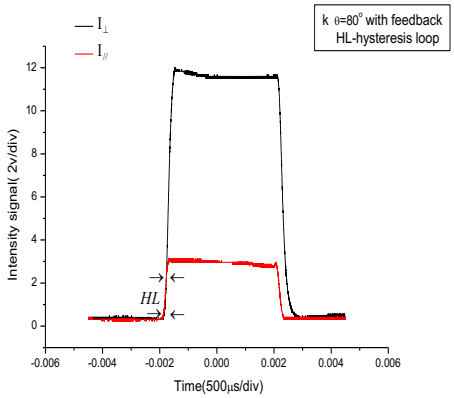

Fig:3.k: $I_{\perp}$ and $I_{//}$ intensity with OFB at θ=80°

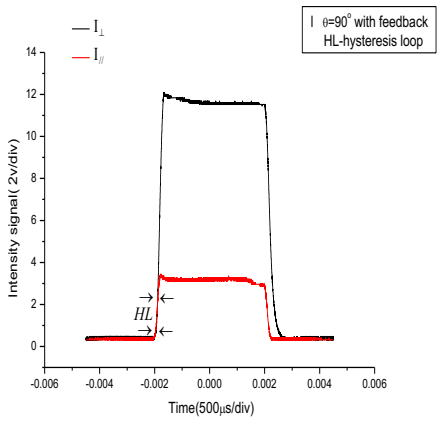

Fig:3.l: $I_{\perp}$ and $I_{//}$ intensity with OFB at θ=90º

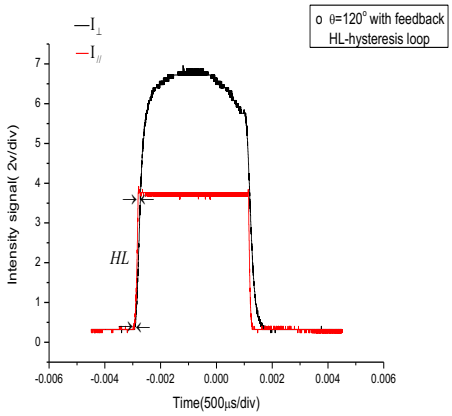

Fig:3.o: $I_{\perp}$ and $I_{//}$ intensity with OFB at θ=120º

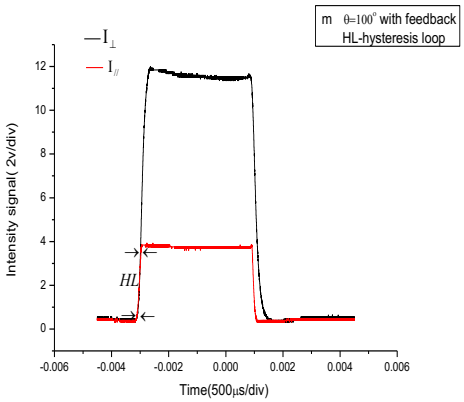

Fig:3.m: $I_{\perp}$ and $I_{//}$ intensity with OFB at θ=100º

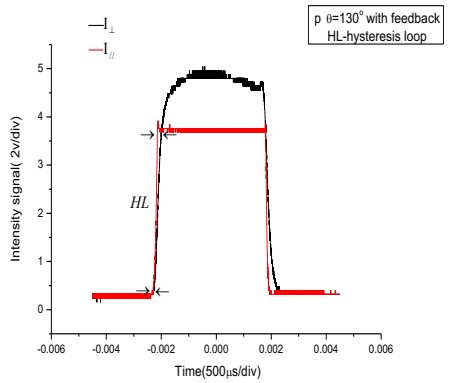

Fig:3.p: $I_{\perp}$ and $I_{//}$ intensity with OFB at θ=130º

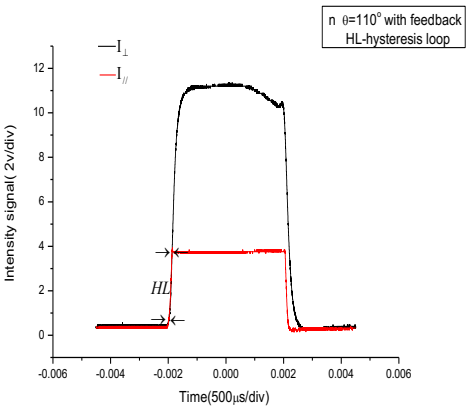

Fig:3.n: $I_{\perp}$ and $I_{//}$ intensity with OFB at θ=110º

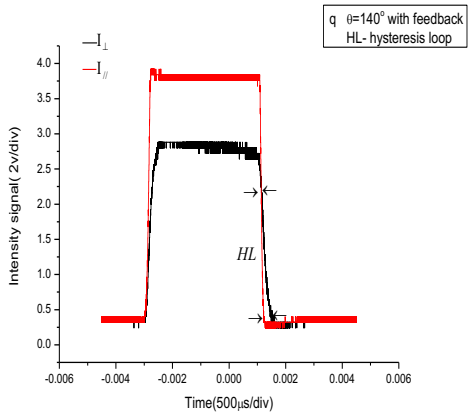

Fig:3.q: $I_{\perp}$ and $I_{//}$ intensity with OFB at θ=140º

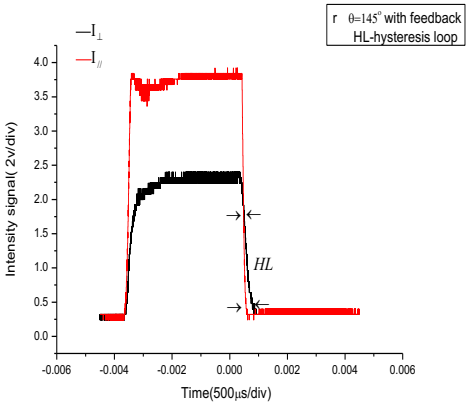

Fig:3.r: $I_{\perp}$ and $I_{//}$ intensity with OFB at θ=145°

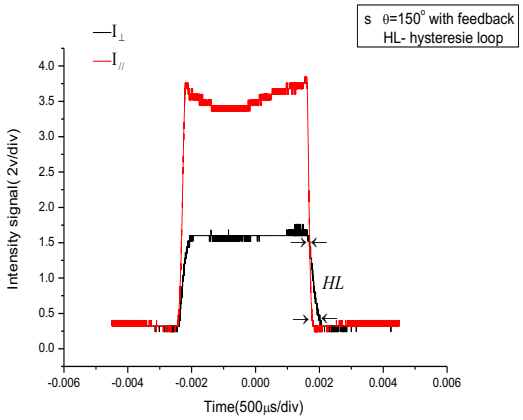

Fig:3.s: $I_{\perp}$ and $I_{//}$ intensity with OFB at θ=150°

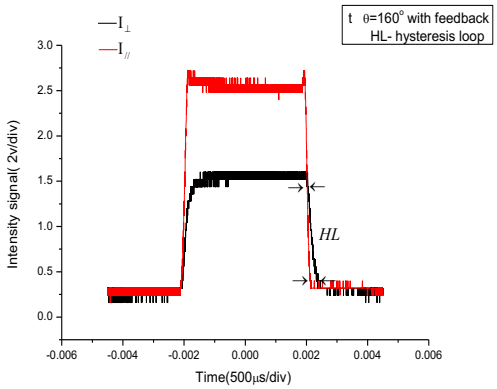

Fig:3.t: $I_{\perp}$ and $I_{//}$ intensity with OFB at θ=160°

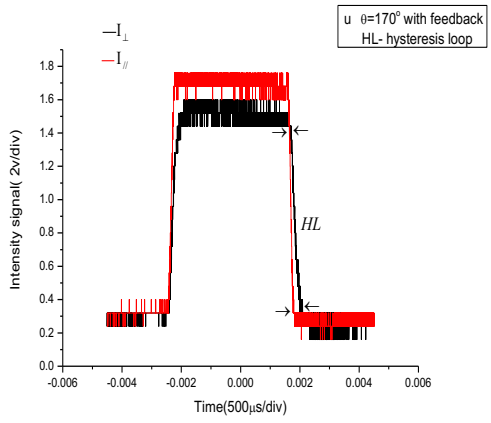

Fig:3.u: $I_{\perp}$ and $I_{//}$ intensity with OFB at θ=170°

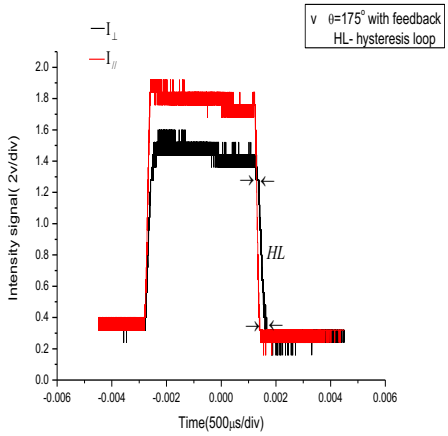

Fig:3.v: $I_{\perp}$ and $I_{//}$ intensity with OFB at θ=175°

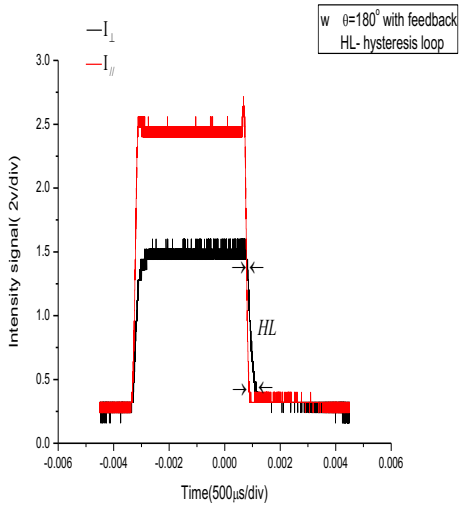

Fig:3.w: $I_{\perp}$ and $I_{//}$ intensity with OFB at θ=180°

4. CONCLUSION

We have shown that hysteresis loop change is caused by using optical feedback. Small hysteresis loop size leads to high intensity for //- or ⊥ polarization and great hysteresis loop size leads to low intensity for //- or ⊥ polarization. The control on hysteresis loop between //- and ⊥ polarization is governed by optical feedback technique. Best results at 70-110 angles, whereas the intensity very high and HL disappear.

REFERENCES

[1] Justin P. and Michael W., 2014, "Physics of Light and Optics", Brigham Young University.

[2] Shulian Z. and Wolfgang H., 2013, "Orthogonal polarization in lasers physical phenomena and engineering applications", John Wiley & Sons Singapore Pte Ltd.

[3] Ropars G., Le Floch A. and Le Naour R., 1992, "Polarization control mechanisms in vectorial bistable lasers for one-frequency systems", Physical Review A, Vol. 6, No. 1, PP. 623-640.

[4] Wu Y., Tan Yi-D., Zhang S.-L. and Li Y., 2013, " Influence of Feedback Level on Laser Polarization in

Polarized Optical Feedback**",** Chinese Physical Letters, Vol. 30, No. 8, PP. 084201-1-4.

[5] Jiyang L., Haisha N. and Yanxiong N., 2017, "Laser feedback interferometry and applications: A review", Optical Engineering, Vol. 56, No. 5, PP. 050901-1-20.

[6] Thomas T., Milan N., Karl B., Yah L. L., Thierry B. and Aleksandar D. R., 2015, "Laser feedback interferometry: A tutorial on the self-mixing effect for coherent sensing", Advances in Optics and Photonics, Vol. 7, PP. 570–631.

[7] Kaiyi Z., Bo G., Yueyue L., Shulian Z. and Yidong T., 2017, "Single-spot two-dimensional displacement measurement based on self-mixing interferometry", Optica, Vol. 4, No. 7, PP. 729–735.

[8] Dongmei G., Haiqing J., Liheng S.and Ming W., 2018, "Laser self-mixing grating interferometer for MEMS accelerometer testing", IEEE Photonics Journal, Vol. 10, No. 1, PP. 1-10.

[9] Rakic A. D., Taimre T., Bertling K., Lim Y. L., Dean P., Valavanis A. and Indjin D., 2019, "Sensing and imaging using laser feedback interferometry with quantum cascade lasers", Applied Physical Review, Vol. 6, PP. 021320-1-19.

[10] Peek H., Bolwijn P. T. and Alkemade T. J., 1967, "Axial mode number of gas lasers from moving-mirror experiments", American Journal of Physics, Vol. 35**,** PP. 820-831.

[11] Paul J. B., 1976, "Laser feedback: its effect on laser frequency", Applied Optics**,** Vol. 15, No. 5, PP. 1119-1120.

[12] Fei L.-G., Zhang S.-L and Wan X.- J., 2004, "Influence of optical feedback from birefringence external cavity on intensity tuning and polarization of laser", Chinese Physical Letters, Vol. 21, No.10, PP. 1944-1947.

[13] WILLIS E. L., JR, 1964, " Theory of an Optical Maser", Physical Review, Vol. 134, No. 6A, PP. A1429-A1450.

[14] Murray S. III, Marlan O. S. and Willis E. L., JR., 1974, "Laser Physics", Addison-Wesley, Reading, MA.

[15] Culshaw W. and Kannelaud J., 1966, "Coherence Effects in Gaseous Lasers with Axial Magnetic Fields. I. Theoretical", Physical Review Vol. 141, No.1, PP.228-236.

[16] Doyle W. M. and White M. B., 1966, "Governing influence of atomic degeneracy on mode interactions in a gas laser", Physical Review Letters, Vol. 17, No. 9, PP. 467-470.

[17] Lett P., Christian W., Surendra S. and Mandel L., 1981, " Macroscopic Quantum Fluctuations and First-Order Phase Transition in a Laser", Physical Review Letters, Vol. 47, No. 26, PP. 1892-1895.

[18] Floch A. L., Ropars G., Lenornamd J. M. and Naour R. L., 1984, "Dynamics of laser eigenstates", Physical Review Letters, Vol. 52, No. 11, PP. 918-921.

[19] Andrew Dienes, 1968, "Theory of Nonlinear Effects in a Gas Laser Amplifier, I. Weak Signals", Physical Review, Vol. 174, No. 2, PP. 400-414**.**

[20] Mao W. and Zhang S.-L., 2006, " Strong optical feedback in birefringent dual frequency laser", Chinese Physics, Vol. 15, No. 2, PP. 340-345.

تأثير حلقة التاخير على شدة الاستقطاب الافقي والعمودي بواسطة التغذية العكسية البصرية.

احسان علي عبد[1،2] و جاسم محمد نجم[1] و سؤدد سلمان احمد[3]

[1] قسم الفيزياء، كلية العلوم، جامعة الانبار / العراق

[2] قسم العلوم الاساسية، كلية طب الاسنان، جامعة الانبار / العراق

[3] قسم الفيزياء، كلية العلوم، جامعة بغداد/ العراق

الخلاصة:

تأثير التغذية العكسية البصرية على حلقة التاخير قد تحقق. تحدث حلقة التاخير بين الحالتين الذاتيتين لليزر هليوم _ نيون وانها تتغير بواسطة التغذية العكسية البصرية عند الزوايا من 0^{o} الى 180^{o} . حجم حلقة التاخير يزداد وينقص مع زاوية تدوير الاستقطاب. حلقة التاخير تؤثر على الاستقطاب العمودي (⊥) والافقي (//) والشدة للحالتين الذاتية. عندما يزداد حجم حلقة التأخير فان الشدة تتناقص (الشدة العمودية او الافقية) والعكس صحيح. أفضل النتائج عند الزوايا من 70^{o}–110^{o} من التجويف الخارجي (تجويف التغذية العكسية البصرية) حيث ان الشدة عالية جدا وحلقة التاخير اختفت.

الكلمات المفتاحية: حلقة التاخير، التغذية العكسية البصرية، الاستقطاب، ليزر هليوم –نيون.